Direct measurement of recurrent fluorescence emission from naphthalene ions

M. Saito [1,2] H. Kubota,[1] K. Yamasa,[1] K. Suzuki,[1] T. Majima [1] and H. Tsuchida[1,2]

[1]*Department of Nuclear Engineering, Kyoto University, Kyoto 615-8540, Japan*
[2]*Quantum Science and Engineering Center, Kyoto University, Uji 611-0011, Japan*

In this study, the recurrent fluorescence of naphthalene ions was investigated using an electrostatic ion beam trap. The number of photons from the recurrent fluorescence on the $D_2 \rightarrow D_0$ transition was measured as a function of time, after the production of naphthalene ions by electron impact. The emission of photons was observed over a time range of approximately 10 ms. The variation in the number of photons for such a long time range could be explained by conducting simulations using previously reported theoretical rate constants of both the fragmentation and the recurrent fluorescence of vibrationally hot naphthalene ions.

I. INTRODUCTION

The processes by which molecules lose their internal energies are called cooling processes. For a polyatomic molecule, an electronically excited energy of the molecule is transferred to the vibrationally excited state of the electronic ground state via internal conversion (IC). In condensed systems, such as solutions, this vibrational energy is subsequently dissipated to the surrounding environment on the order of picoseconds, resulting in rapid cooling of the molecules. However, under high-isolation conditions, because there is no interaction with the surroundings, two competing processes, as displayed in Fig. 1, are mainly involved in the loss of the internal energy [1,2]. The first process is the vibrational radiative cooling by infrared photon emission. The second is the fragmentation of molecules possessing internal energies higher than the threshold level of the fragmentation. In 1988, Léger *et al.* proposed an additional radiative cooling process for isolated molecules [3], in which the vibrationally hot molecule in the electronic ground state is converted again to an electronically excited state by the reverse process of IC. Subsequently, the molecule is cooled by fluorescence emission. This fluorescence emission following the inverse IC (IIC) is called the recurrent fluorescence (RF). From the theoretical calculations of polycyclic aromatic hydrocarbon (PAH) ions [1], in the case of high internal energy, the time constant of the cooling by RF is expected to be significantly smaller than that by infrared radiation, indicating that the radiative cooling is governed by the RF process. The study of radiative cooling by RF is important not only to clarify the deexcitation process unique to isolated molecules but also to investigate the formation processes of isolated molecules in outer space. This is because the cooling by the RF process is expected to competitively suppress the decomposition of high-internal-energy molecules.

Recent developments in the technique of storing ions in electrostatic devices allow the confinement of polyatomic molecular ions in ultrahigh vacuum and the observation of the cooling processes of isolated macromolecular ions for a long time [4]. The RF cooling of PAH ions (anthracene and naphthalene ions) was experimentally confirmed by Martin *et al.* for the first time using an electrostatic ion storage ring [5–7]. In these experiments, they derived the temporal change in the internal energy distribution of the stored vibrationally hot ions by measuring the neutral particles generated from their fragmentation. Accordingly, they confirmed that the cooling attributed to RF is the dominant process in radiative cooling. Recently, Ebara *et al.* reported the successful direct detection of emitted RF photons for C_6^- cluster ions stored in an electrostatic storage ring [8]. However, the direct detection of RF photons for other polyatomic molecules, including the PAH ions that have been investigated from the start, is not yet known. Therefore, detailed information of RF is required.

In this study, we succeeded in directly observing the RF from naphthalene ions confined in an electrostatic ion beam trap. This trap has been employed to measure the emitted photons during the decay of metastable levels of rare gas ions [9–11]. The counting rate of the RF photons emitted from the naphthalene ions was measured as a function of time up to the order of 10 ms, which is quite a long time. The obtained time spectrum was compared to that derived by simulation using the theoretical data related to the cooling of vibrationally hot molecules. In addition, the wavelength dependence of the yield of the RF photons was measured and compared to the previously reported photoabsorption spectrum of naphthalene ions.

II. EXPERIMENT

The experiments were performed at the Quantum Science and Engineering Center of Kyoto University using an electrostatic ion beam trap. The experimental setup and procedures were similar to those described previously [10]. Figure 2 schematically displays the setup of this experiment. Excited positive naphthalene ions ($C_{10}H_8^+$) were generated in a Nier-type electron impact ion source. Ar gas was fed along with sublimated naphthalene gas into the ion source, to prevent clogging of the gas feed pipe. The produced ions were extracted from the ion source at an extraction voltage of 1.2 kV. The ion beam was focused by an einzel lens and
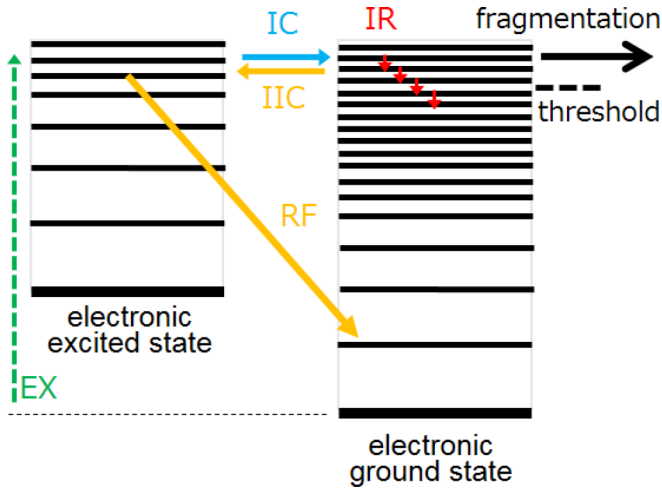
FIG. 1. Schematic of the energy-level diagram. IC, internal conversion; IIC, inverse internal conversion; IR, infrared radiation; RF, recurrent fluorescence; EX, excitation.

was chopped to a desired time width using an electrostatic chopper. Subsequently, the masses and charges of the ions were analyzed in a 45° analyzing magnet, and $C_{10}H_8^+$ ions were injected into the trap through a 40-mm-long pipe with an internal diameter of 4 mm. The latter limited the conductance of the gas flow from the beam line into the trap. The flight time of the ions from the ion source to the trap center was 41 μs, which was sufficiently shorter than the order of the expected RF time (on the order of milliseconds [7]).

A detailed description of the trap can be found in our previous paper [12]. In brief, the trap consisted of two sets of cylindrical electrodes that functioned as reflectors and einzel lenses. The space between two lenses was a field-free region. The potentials on the reflector electrodes on the entrance side were initially kept at zero. After the injection of an ion bunch, these potentials were rapidly increased within 600 ns using fast high-voltage switches. This rise time was much shorter than the circulation time of the $C_{10}H_8^+$ ions in the trap ($\sim$19 μs). Potentials were continuously applied to the reflector electrodes on the exit side, and the injected ions were reflected multiple times between the two reflectors along the trap axis and were stored in the trap. The storage time of the ions was limited by the collisions with the residual gases.
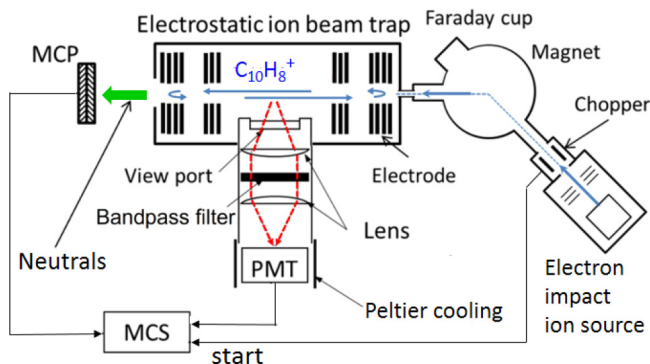

FIG. 2. Schematic view of the experimental setup.

The trap was evacuated using a turbomolecular pump (900 l/s) and a nonevaporable getter pump (100 l/s for H_2). The base vacuum pressure in the trap chamber was maintained at 2×10^{-7} Pa, which allowed the storage of the $C_{10}H_8^+$ ions for approximately 500 ms.

Following the achievement of the confinement of the $C_{10}H_8^+$ ions, the photons emitted from the ions were measured at the center of the field-free region of the trap, as depicted in Fig. 2. The emitted photons were observed from a direction perpendicular to the trapped ion beam using a sapphire viewport, and were focused on the detection plane (5-mm diameter) of a cooled photomultiplier tube (PMT) (H7421-40, Hamamatsu Photonics) using two lenses. This PMT is sensitive to wavelengths from 300 to 710 nm, with a peak counting efficiency of 30% at 530 nm. The dark noise of the PMT was approximately 9 counts/s when it was cooled to $-10\,^{\circ}$C. Initially, using this optical system, we detected RF photons at around 674 nm (1.84 eV), corresponding to the energy of the lowest allowed electronic transition to the ground state ($D_2 \rightarrow D_0$) of $C_{10}H_8^+$ ions [13,14]. The first electronically excited level in $C_{10}H_8^+$ was a metastable state; hence, the transition of $D_1 \rightarrow D_0$ was forbidden. The shorter side of the wavelength range was selected using a long-pass filter (>575 nm) and the longer side was limited by the sensitivity of the PMT ($< \sim 700$ nm). The detection efficiency of the optical system of the wavelength at 674 nm was 6.2×10^{-3} for the emitted photons. This was approximately estimated using the following data of the manufacturers: transmittance of the viewport, 0.85; lens, 0.95; and filter, 0.94; counting efficiency of the PMT, 0.18; and solid angle of the lens, 0.59 sr. In the succeeding experiments, we performed a series of measurements using some narrow-bandpass filters, to determine the wavelength dependence of the RF in detail. Subsequently, the PMT was replaced by one having a sensitivity for wavelengths up to 880 nm (H7421-50). The transmission wavelength of each bandpass filter and the estimated detection efficiency are listed in Table I. The photon counts were recorded by a multichannel scaler (MCS), with a dwell time of 1.6 μs, from the beginning of the beam chopping. The sweep time of the MCS was 100 ms. Following one sweep, the ions were dumped from the trap by switching off the voltages on the entrance side. The cycle of ion injection, trapping, and dumping was repeated at 10 Hz, and data were collected for over 10^5 injections.

Neutral particles escaping from the trap originated partly from the collisional dissociation or neutralization of the $C_{10}H_8^+$ ions by the residual gases and partly by the spontaneous dissociation of the hot $C_{10}H_8^+$ ions as described in the next section. The neutrals were measured using a microchannel plate installed downstream of the trap. The counts of the neutrals were monitored using a rate meter, to appropriately align the incident beam to the trap axis. They were recorded in the MCS simultaneously with the photon measurement, to normalize the number of stored ions at each measurement with a different bandpass filter.

III. RESULTS AND ANALYSIS

Figure 3(a) presents the photon counts as a function of time, as obtained from 2.6×10^6 storage cycles of a bunch beam chopped to a width of approximately 7 μs. It can be

TABLE I. Transmission wavelengths of the used bandpass filters. The detection efficiency was estimated at the center transmission wavelength of each filter. PMT: used photomultiplier, -40: H7421-40; -50: H7421-50. In the case of 684 nm, measurements using H7421-40 and -50 were individually performed for the normalization.

Transmission wavelength (nm)		Detection efficiency	PMT
Center	Width	$(\times 10^{-3})$	
562	40	10	−40
607	36	9.3	−40
650	40	8.1	−40
684	24	5.3, 3.7	−40, −50
725	40	3.7	−50
775	50	3.7	−50
825	50	3.4	−50

clearly seen that the photon counts oscillate with a constant period. The average oscillation period obtained from the spectrum is 9.5 μs. This value is consistent with half of the circulation time of 1.2-keV $C_{10}H_8^+$ ions in the trap simulated using the SIMION software [15], proving that the detected photons are from the stored 1.2-keV $C_{10}H_8^+$ ions. As for the shape of the initial few peaks, the peak tails appear to extend toward the longer time period, as clearly seen in the second peak. This behavior probably results from ions that were injected into unstable orbits at an angle larger than the acceptance angle of the trap and were lost from the trap in such a fast time, especially after the first reflection.

To obtain data with better statistics and investigate the time dependence of the RF, the photon count spectrum was measured for the injection of a bunch beam with a relatively longer time width (~ 19 μs) than previously. Figure 3(b) displays the results for 5.7 $\times 10^5$ storage cycles of the bunch beam. A gradual decrease in the photon counts with time can be observed in the spectrum, which is superimposed on a constant background. The count rate of this background (~ 8 cps) is very close to the dark count rate of the PMT, indicating that the background is mostly due to the dark noise of the PMT.

As depicted in Fig. 3(b), the fluorescence emission from the $C_{10}H_8^+$ ions is remarkable, even after 10 ms. The Einstein coefficient for the spontaneous electronic transition between the $D_2(^2B_{2g})$ and $D_0(X^2A_u)$ states is estimated as 1.6×10^6 s^{-1} from the theoretical electronic transition energy of 1.89 eV and oscillator strength of 4.2×10^{-2} [13]. This yields a fluorescence time of the order of less than 1 μs, which is much shorter than the flight time of the ions from the ion source to the trap. However, the fluorescence time in Fig. 3(b) is approximately three orders of magnitude longer, suggesting that our observed fluorescence is not a spontaneous fluorescence of electronically excited ions but that emitted by the IIC process. In fact, it was recently reported that the internal energies of $C_{10}H_8^+$ ions confined in an ion storage ring were cooled to the order of milliseconds owing to the RF process [7].

Figure 3(c) shows the counts of the neutral particles, measured simultaneously with the photon spectrum in Fig. 3(b). Similar to the photon spectrum, the clear decrease of the counts is seen at shorter times ($< \sim 10$ ms). This decrease results from the spontaneous decay of hot naphthalene ions, as discussed for the neutral time spectra of other molecular ions such as anthracene ions [5] and amino acid ions [16]. On the other hand, a slow exponential decrease of the counts is observed above 10 ms, as indicated by the exponential curve fitted to the data. The time constant of this exponential decay changes depending on the vacuum pressure in the trap, suggesting that the neutral particles in this time range are generated dominantly by collisions with residual gases. The low counts observed at longer times (>88ms) are the dark counts of the MCP.

Figure 4 presents the relative yield of the photons as a function of wavelength, measured using previously mentioned narrow-bandpass filters in the range of 542–850 nm. Except for replacing the bandpass filter, the experimental conditions are the same as those in Fig. 3(b). The measured yield begins to increase at around 560 nm, reaches a peak at 670–700 nm, and then decreases gradually toward 800–850 nm. It should be mentioned that the count rate above the background level was not observed using another filter with shorter neighboring wavelength range (300–550 nm). The photoabsorption spectrum of the $C_{10}H_8^+$ ions [13] is also plotted with a broken line for comparison. The peaks in the photoabsorption spectrum correspond to the absorption band of the $D_0 \rightarrow D_2$ transition of the $C_{10}H_8^+$ ions. Our observed peak wavelength is very similar to that in the photoabsorption spectrum, thus verifying that the photons emitted by the $D_2 \rightarrow D_0$ transition are detected. The shape of the peak in our measurement is apparently broadened to longer wavelengths than that of the photoabsorption spectrum. This may be partly because the referred absorption spectrum was measured for the $C_{10}H_8^+$ ions cooled to 12 K and partly because of the small Stokes shift and mirror image relation between the absorption and fluorescence spectra. In Stokes shift, the fluorescence has a lower energy than the absorbed photon, because of the rapid nonradiative decay of a high vibrational level in the electronically excited state [17]. Until now, observations of the Stokes shifts for other type of organic molecular ions in the gas phase have been reported [18].

To understand the observed time spectrum [Fig. 3(b)] quantitatively, we simulated the counts of the RF photons as a function of time using previous data [1,19,20]. The rate equation for $C_{10}H_8^+$ ions with internal energy E in the
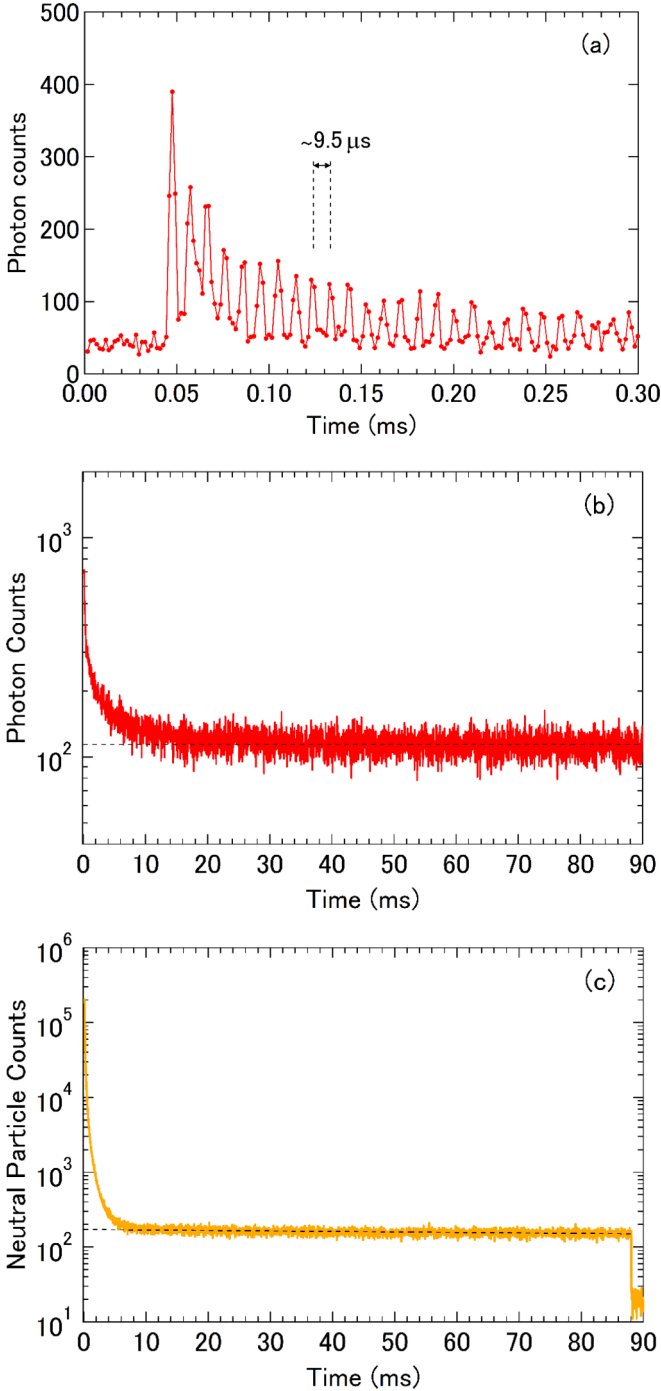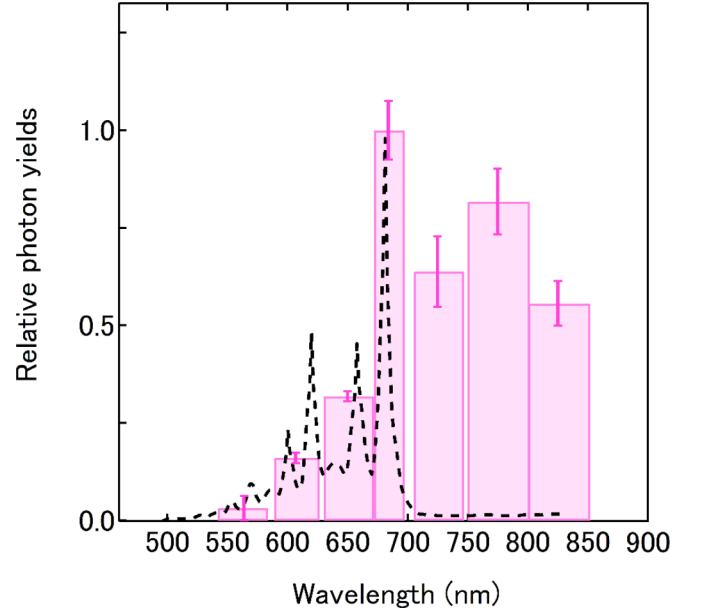
FIG. 4. Relative yields of the RF photons as a function of the photon wavelength, which are obtained from separate measurements using different bandpass filters, as listed in Table I. The difference in the number of stored ions of different measurements was normalized using the counts of neutrals recorded in the MCS simultaneously with the counts of photons, as shown in Fig. 3(c). Other experimental conditions were the same for each measurement. The photoabsorption spectrum of $C_{10}H_8^+$ ions taken from [13] is also drawn with a broken line for comparison.

FIG. 3. Photon counts for the wavelength range of 575–700 nm as a function of time. A beam chopped to a width of (a) 7 μs or (b) 19 μs was injected into the trap. The dwell time of the MCS was set to (a) 1.6 μs and (b) 26 μs. A broken line in (b) shows the background count determined by averaging the counts for $t > 20$ ms. (c) Counts of the neutral particles as a function of time measured simultaneously with (b). The broken line in (c) is the exponential function fitted to the data from 15 to 85 ms. The stored ions were released from the entrance of the trap at 88 ms.

electronic ground state is given by

$$\frac{dN(E,t)}{dt} = -[k_{FR}(E) + k_{RF}(E) + k_{IR}(E)]N(E,t)$$
$$+ k_{IR}(E')N(E',t), \qquad (1)$$

where $k_{FR}(E)$, $k_{RF}(E)$, and $k_{IR}(E)$ are the energy-dependent rate constants of the fragmentation, electronic transition via RF emission, and vibrational transition via infrared (IR) emission, respectively. The last term is the rate of generations of ions with E by the vibrational transition from a higher internal energy, E'. The rate constant, $k_{IR}(E)$, of the IR emission was found to be almost independent of energy E and was one to two orders of magnitude smaller than $k_{RF}(E)$ in the energy range discussed hereafter [1]. For simplicity, assuming that the contribution of the IR emission terms in Eq. (1) is negligibly small, the number of the $C_{10}H_8^+$ ions with internal energy E at a time t is given by

$$N(E,t) = N(E,t=0)\exp\{-[k_{FR}(E) + k_{RF}(E)]t\}$$
$$\propto f(E)\exp\{-[k_{FR}(E) + k_{RF}(E)]t\}, \qquad (2)$$

where $f(E)$ denotes the initial internal energy distribution (IED) of the $C_{10}H_8^+$ ions produced by electron impact (at $t = 0$). $k_{RF}(E)$ is the sum of the rate constant of the RF from the ith electronic excited state: $k_{RF}(E) = \sum_i k_{RF}^i(E)$. When the RF photons are those emitted by the $D_i \rightarrow D_0$ transition, the observed counts at t, $C_{RF}^i(t)$, are expressed as

$$C_{RF}^i(t) \propto \int_E k_{RF}^i(E)f(E)\exp\{-[k_{FR}(E) + k_{RF}(E)]t\}dE. \qquad (3)$$

To generate the photon time spectrum of the present case ($i = 2$) from Eq. (3), the values of the following terms were used in our calculation: for rate constants, the theoretical values of $k_{FR}(E)$ [19] and $k_{RF}(E)$ of $C_{10}H_8^+$ [1], obtained
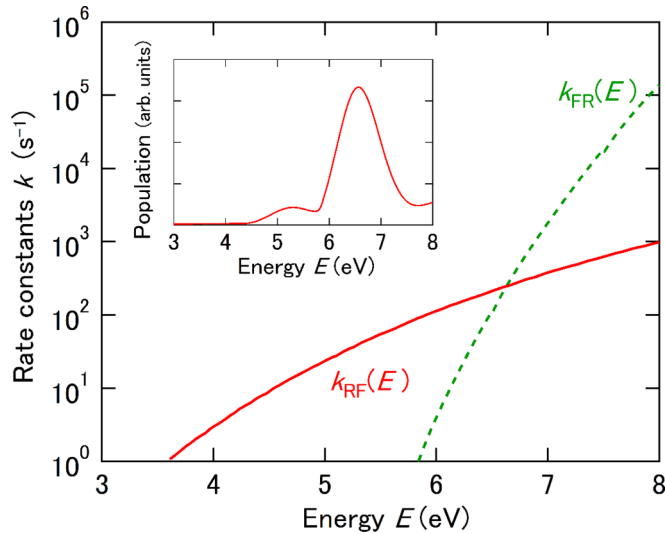
FIG. 5. Theoretical rate constants of the (a) dissociation, $k_{FR}(E)$ (Fig. 4 in [19]), and (b) the recurrent fluorescence, $k_{RF}(E)$(Fig. 3(c) in [1]) for the $C_{10}H_8^+$ ions as a function of internal energy E are drawn by solid and dotted curves, respectively. The inset displays the calculated internal energy distribution of the $C_{10}H_8^+$ ions when produced in the ion source. The large peak at $\sim$6.5 eV is attributed to the $S_0 \rightarrow S_2$ transition of the naphthalene molecules, whereas the small peak at $\sim$5.2 eV is attributed to the $S_0 \rightarrow S_1$ transition [20]. The details of the calculation are described in the text.

from statistical reaction rate models using the quantum-chemically calculated vibrational level density of $C_{10}H_8^+$, were employed (see Fig. 5). This theoretical $k_{RF}(E)$ was previously reported to be coincident with the experimentally derived $k_{RF}(E)$ for the IED of 5.5–6 eV [21]. In the calculation, $k_{RF}^{i=2}(E)$ was treated as $k_{RF}^{i=2}(E) \approx k_{RF}(E)$ because, in the case of $C_{10}H_8^+$, $k_{RF}^i(E)$ decreases rapidly as the electronically excited state, i, increases. The contribution of the lines higher than the transition from the $i = 2$ state, $\sum_{i>2} k_{RF}^i(E)$, is estimated to be less than 1% of $k_{RF}(E)$ [1,22,23]. For the IED, $f(E)$ was not measured in this experiment, and its data could not be found in previous literature. The IED of the naphthalene molecules before the electron impact in the ion source, $f'(E_0)$, was determined by assuming a Boltzmann-type distribution for the measured temperature of the ion source (573 K). When the internal energy was increased by the electron impact from E_0 to $E = E_0 + \varepsilon$, $f(E)$ is given by the following convolution integral:

$$f(E) = \int f'(E - \varepsilon)g(\varepsilon)d\varepsilon, \tag{4}$$

where $g(\varepsilon)$ is the distribution of the deposited energy, ε, by the electron impact. For $g(\varepsilon)$, we employed an energy-loss distribution of 100-eV electrons colliding with naphthalene molecules [20], such that it is similar to previous photoabsorption results [24]. This treatment assumes that the internal energy of a naphthalene molecule is increased by the collision with an electron and the following IC process, and the subsequent collision by another electron ionizes the hot molecule. The calculated IED, $f(E)$, is presented in the inset of Fig. 5. It has a dominant peak at $\sim$6.5 eV, where the magnitude of
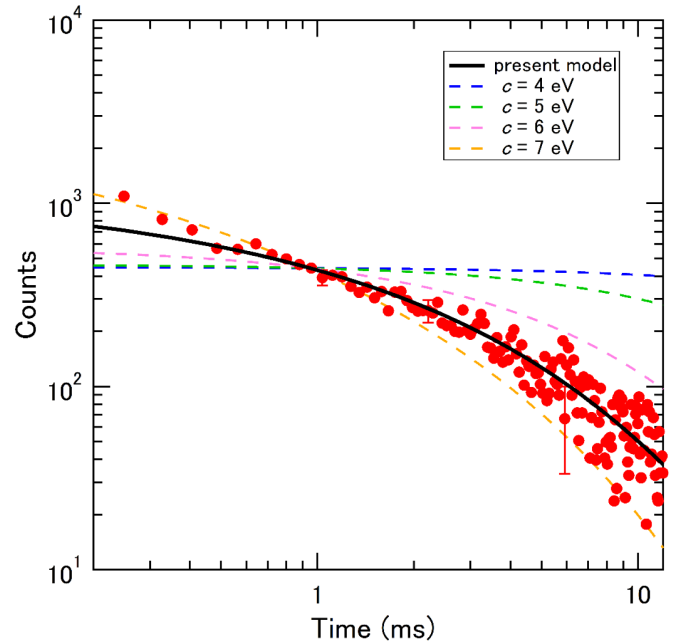

FIG. 6. Comparison of the measured time evolution of the photon counts (circles) with the simulation results (solid line). The experimental data are subtracted with the dark noise counts and are combined into time bins of 78 μs. Typical experimental errors are also shown. The errors at a fast time ($<$1 ms) are within the circle size. The broken lines are the simulation results, assuming the internal energy distributions of Gaussian type of 1 eV width centered at c = 4, 5, 6, and 7 eV. The simulation results are normalized to the experimental data at 1 ms.

the theoretical $k_{RF}(E)$ is comparable to that of the theoretical $k_{FR}(E)$ as can be seen from Fig. 5. Finally, using Eq. (3), the contribution of the ions with energy E of more than 8 eV is negligibly small ($<$0.2%), because such ions mostly decay before entering the trap at $\sim$40 μs owing to the large $k_{FR}(E)$ and $k_{RF}(E)$.

The simulated time evolution of the photon count rate is displayed by the solid curve in Fig. 6. The experimental data with the background subtracted are also plotted for comparison. The simulation results are normalized to the experimental data at 1 ms. As shown in the figure, the simulation reproduces our data well for the long time range (0.5–10 ms). The broken lines are the results of the Gaussian IEDs of 1 eV width centered at 4, 5, 6, and 7 eV, to see the sensitivity of the model with respect to the actual IED. The simulated curve clearly changes with the 1-eV shift of the IED, as demonstrated by the broken lines. The solid curve fits the experimental data best, suggesting that the IED model shown in Fig. 5 will be close to the actual IED. For time less than 0.4 ms, the experimental results decrease more rapidly than the solid curve. The reason for this discrepancy in the slope remains unclear; however, we interpret that the actual rate constants are larger than the employed theoretical ones, particularly at the higher-energy side of the IED. It could also be that the distribution in Fig. 5 underestimates the actual IED on the high-energy side, especially around 7 eV, as suggested by the simulation result for the Gaussian IED centered at 7 eV.

IV. SUMMARY

In this study, we measured the number of emitted photons in the $D_2 \rightarrow D_0$ transition of excited naphthalene ions confined in an electrostatic ion beam trap as a function of time. Photons were observed on the order of milliseconds; this timescale is much longer than that for the spontaneous fluorescence of electronically excited naphthalene ions. The photon yields as a function of the wavelength were compared to the experimental photoabsorption spectrum for the absorption band of the $D_0 \rightarrow D_2$ transition of naphthalene ions, and it was confirmed that the peak wavelengths of both the spectra agreed well. The observed phenomenon was attributed to recurrent fluorescence, which is the emission of photons from the excited electronic state following an inverse internal conversion process. This is a direct observation of recurrent fluorescence photons for a long time (over $\sim$10 ms). The time dependence of the number of emitted photons was simulated using previously reported theoretical rate constants of the fragmentation and recurrent fluorescence of naphthalene ions as a function of their internal energy. The simulation reproduced well the present experimental data in the observed time range except below $\sim$0.4 ms. This study provided precise experimental information regarding the recurrent fluorescence by direct and long-time observations of emitted photons from this process. It also demonstrated that the electrostatic ion beam trap is a suitable tool to the study the cooling of isolated molecular ions by fluorescence measurements.

[1] P. Boissel, P. de Parseval, P. Marty, and G. Lefevre, J. Chem. Phys. **106**, 497 (1997).

[2] A. Léger, P. Boissel, F. X. Désert, and L. d'Hendecourt, Astron. Astrophys. **213**, 351 (1989).

[3] A. Léger, P. Boissel, and L. d'Hendecourt, Phys. Rev. Lett. **60**, 921 (1988).

[4] L. H. Andersen, O. Heber, and D. Zajfman, J. Phys. B: At., Mol. Opt. Phys. **37**, R57 (2004).

[5] S. Martin, J. Bernard, R. Brédy, B. Concina, C. Joblin, M. Ji, C. Ortega, and L. Chen, Phys. Rev. Lett. **110**, 063003 (2013).

[6] S. Martin, M. Ji, J. Bernard, R. Brédy, B. Concina, A. R. Allouche, C. Joblin, C. Ortega, G. Montagne, A. Cassimi, Y. Ngono-Ravache, and L. Chen, Phys. Rev. A **92**, 053425 (2015).

[7] S. Martin, J. Matsumoto, N. Kono, M.-C. Ji, R. Brédy, J. Bernard, A. Cassimi, and L. Chen, Nucl. Instrum. Methods Phys. Res., Sect. B **408**, 209 (2017).

[8] Y. Ebara, T. Furukawa, J. Matsumoto, H. Tanuma, T. Azuma, H. Shiromaru, and K. Hansen, Phys. Rev. Lett. **117**, 133004 (2016).

[9] K. G. Bhushan, H. B. Pedersen, N. Altstein, O. Heber, M. L. Rappaport, and D. Zajfman, Phys. Rev. A **62**, 012504 (2000).

[10] M. Saito, N. Ojima, S. Itoi, and Y. Haruyama, Phys. Rev. A **91**, 012508 (2015).

[11] M. Saito, A. Chikaoka, T. Majima, M. Imai, H. Tsuchida, and Y. Haruyama, Nucl. Instrum. Methods Phys. Res., Sect. B **414**, 68 (2018).

[12] T. Ota, M. Saito, A. Yokota, and Y. Haruyama, Jpn. J. Appl. Phys. **45**, 5263 (2006).

[13] T. Bally, C. Carra, M. P. Fülscher, and Z. Zhu, J. Chem. Soc., Perkin Trans. 2, 1759 (1998).

[14] F. Salama and L. J. Allamandola, J. Chem. Phys. **94**, 6964 (1991).

[15] D. A. Dahl, Int. J. Mass Spectrom. **200**, 3 (2000).

[16] J. U. Andersen, H. Cederquist, J. S. Forster, B. A. Huber, P. Hvelplund, J. Jensen, B. Liu, B. Manil, L. Maunoury, S. B. Nielsen, U. V. Pedersen, H. T. Schmidt, S. Tomita, and H. Zettergren, Eur. Phys. J. D **25**, 139 (2003).

[17] J. R. Lakowicz, in *Principles of Fluorescence Spectroscopy*, 3rd ed. (Springer, New York, 2006), p. 6.

[18] Q. Bian, M. W. Forbes, F. O. Talbot, and R. A. Jockusch, Phys. Chem. Chem. Phys. **12**, 2590 (2010).

[19] E. A. Solano and P. M. Mayer, J. Chem. Phys. **143**, 104305 (2015).

[20] K. H. Huebner, S. R. Mielczare, and C. E. Kuyatt, Chem. Phys. Lett. **16**, 464 (1972).

[21] C. Ortéga, R. Brédy, L. Chen, J. Bernard, M. Ji, G. Montagne, A.R. Allouche, A. Cassimi, C. Joblin, and S. Martin, J. Phys.: Conf. Ser. **583**, 012038 (2015).

[22] F. Pauzat, D. Talbi, M. D. Miller, D. J. De Frees, and Y. Ellinger, J. Phys. Chem. **96**, 7882 (1992).

[23] O. Parisel, G. Berthier, and Y. Ellinger, Astron. Astrophys. **266**, L1 (1992).

[24] G. A. George and G. C. Morris, J. Mol. Spectrosc. **26**, 67 (1968).